ORIGINAL ARTICLE

J Bacteriol Virol. Vol 54. No 1. March 2024; 54(1): 50-61
https://doi.org/10.4167/jbv.2024.54.1.050
pISSN 1598-2467 / eISSN 2093-0429

JBV

Saucernetin-8 from *Schisandra chinensis* as a Potent Antiviral Agent Against Coxsackievirus B3

Hwa-Jung Choi*

Department of Beauty Art, 142 Bansong Beltway (Bansong-dong), Youngsan University, Busan 48015, Republic of Korea

Corresponding
Hwa-Jung Choi, PhD
Department of Beauty Art, 142 Bansong Beltway (Bansong-dong), Youngsan University, Busan 48015, Republic of Korea
Phone : +82-51-540-7235
E-mail : rerived@ysu.ac.kr

Received : March 23, 2024
Revised : April 2, 2024
Accepted : April 3, 2024

Various plants have been studied for their therapeutic potential to treat virus-induced diseases. This study aimed to investigate in vitro anti-coxsackievirus B3 (CVB3) effect of saucernetin-8 isolated from *Schisandra chinensis* and mode of its action. The action of saucernetin-8 on CVB3 proliferation, the effect of saucernetin-8 on VP3 protein, mitochondrial reactive oxygen species (mtROS) and expression levels of STING/p-STING/IRF3/p-IRF3 were investigated by RT-qPCR, immunofluorescence and Western blot. Saucernetin-8 exhibited over 60% inhibition of CVB3-induced cytotoxicity at a concentration of 0.4 μg/mL. Saucernetin-8 completely suppressed viral genome replication at a concentration of 10 μg/mL. Furthermore, saucernetin-8 inhibited the expression of VP3, the capsid protein of CVB3, by approximately 50% at a concentration of 10 μg/mL. Immunofluorescence assay showed that saucernetin-8 inhibited VP3 expression by approximately 50%. Saucernetin-8 increased mtROS levels in CVB3-infected Vero cells. The STING/IRF3 pathway is activated in cells treated with saucernetin-8. Therefore, saucernetin-8 is a candidate for development of antivirals against CVB3.

Key Words: Coxsackievirus B3, Saucernetin-8, Antiviral activity, Mitochondria reactive oxygen species

No potential conflict of interest relevant to this article was reported.

INTRODUCTION

Hand-foot-and-mouth disease (HFMD) is caused by human enteroviruses (EVs) and EVs were initially classified into poliovirus (PV), echo, coxsackievirus (CV)-A and B, and emerging EVs (1). HFMD, an acute viral contagion, has triggered extensive outbreaks across Asia over the last ten years. It typically presents with mild to moderate symptoms, including fever, mouth sores, and rashes on the hands and feet. In its more severe form, the illness can affect the nervous system, leading to symptoms associated with respiratory and circulatory disruption (2). CVB3 is frequently recognized as the primary causative agent of myocarditis in developed countries (3, 4). Lymphocytic myocarditis, characterized by cardiac necrosis, stands as the predominant viral myocarditis variant in humans. This condition can manifest as either a self-limited acute disease or as a perilous, fulminant myocarditis version. It is known to induce left ventricular dysfunction and heart failure, with a subset of patients potentially progressing to dilated cardiomyopathy (DCM) (5-7).

Mitochondria utilize reactive oxygen species (ROS) as signals to adapt to heightened energy requirements, altering the composition and organization of the mitochondrial electron transport chain (ETC) or enhancing mitochondrial biogenesis, known as reactive biogenesis (8). Furthermore, mitochondrially generated ROS has health-promoting effects known as mitohormesis (9). Interactions between viruses and mitochondrial membranes, along with other components associated with mitochondria, result in a rise in ROS production. The strategic manipulation of apoptosis triggered by virus-induced mitochondrial ROS (mtROS) serves as a critical viral tactic for enhancing intracellular replication and ensuring the timely release of viral offspring (10).

Schisandra chinensis Turcz. (Baill.), a member of the *Schisandraceae* family, originates from northeastern Korea, Japan, China, Manchuria, and Russia's Far Eastern regions (11). This plant enhances immune function, serves as a tonic, and displays antioxidant, anti-inflammatory, antiviral, anticancer, anti-aging, antidiabetic activities, along with offering protection for the liver and skin (12, 13).

In this study, we examined the antiviral activity of saucernetin-8, an active compound isolated from *S. chinensis* against CVB3. In addition, to further elucidate the action of saucernetin-8 on CVB3 proliferation, the effect of saucernetin-8 on VP3 protein, mtROS and expression levels of STING/p-STING/IRF3/p-IRF3 were investigated through RT-qPCR, immunofluorescence, and Western blot.

MATERIALS AND METHODS

Extraction and Isolation

S. chinensis powder was soaked in 3 L of methanol for 3 days at room temperature and then filtered (Whatman No. 2). This process was repeated three times using 3L of methanol, and the filtrate was evaporated using a 40℃ water bath to obtain a dark green residue after removing the solvent using a rotary evaporator. The entire residue was dissolved in 1L of water, and then n-hexane, ethyl acetate (EtOAc), and n-butanol were sequentially distributed. Since the EtOAc fraction exhibited the highest antiviral activity against CVB3 among the three fractions, reversed-phase column chromatography (Merck, 40-63 μm, 300 g) was performed, eluting with a gradient consisting of methanol : water to yield 10 subfractions (2:8, 4:6, 6:4, 8:2, 10:0; 2 × 500 mL each). Among the fractions based on bioassay-based classification, fraction 7, which showed the strongest inhibitory effect, was analyzed by column chromatography. The active compound was isolated from Fraction 7 through purification using preparative HPLC. This process employed a gradient ranging from 30% to 100% acetonitrile in water, utilizing a Shiseido-Capcell Pak C18 UG120 column (250 × 10 mm, 10 μm, Japan) (S. Fig. 1). The structure of active compound was confirmed by the spectroscopic experiments including of UV, EI-MS, ^{1}H-NMR, and ^{13}C-NMR. The nuclear resonance signals of ^{1}H-NMR, and ^{13}C-NMR of active compound was identified with saucernetin-8 (S. Fig. 2).

Cell culture and viruses

1×10^{3} PFU CVB3 (obtained from the American Type Culture Collection, Manassas, USA, ATCC no. VR-30) were propagated at 37℃ in Vero cells (ATCC), a kidney epithelial cell line originally derived from an African green monkey. Vero cells were cultured in Dulbecco's Modified Eagle Medium (DMEM) supplemented with 10% heat-inactivated fetal bovine serum and 0.01% antibiotic-antimycotic solution, in a 37℃ incubator with 5% CO2 (SANYO Electric Co., Osaka, Japan). The antibiotic-antimycotic solution, trypsin-EDTA, fetal bovine serum, and DMEM were provided by Corning (Corning Incorporated, New York, USA), and tissue culture plates were purchased from Falcon (BD Biosciences, New Jersey, USA).

Antiviral activity assay

Antiviral activity and cytotoxicity assays were conducted using the Sulforhodamine B (SRB) assay method to assess

cytopathic effect (CPE). A day prior to infection, Vero cells were seeded at a density of 3×10^4 cells per well in a 96-well culture plate. The following day, the culture medium was removed, and cells were washed with 1× phosphate-buffered saline (PBS) (Corning Incorporated, New York, USA). The infectivity of each virus was assessed by monitoring CPE using the SRB method, enabling determination of cell viability percentage. Diluted virus suspension of CVB3 was added to mammalian cells at a dose ensuring appropriate CPEs at 48 hours post-infection. Antiviral activity of each test compound was assessed with 5-fold diluted concentrations ranging from 0.4 μg/mL to 10 μg/mL. Virus controls (virus-infected, non-drug-treated cells) and cell controls (non-infected, non-drug-treated cells) were each plated in triplicate. Rupintrivir and sulforhodamine B (SRB) were procured from Sigma-Aldrich (Sigma Aldrich, Massachusetts, USA). Following incubation at 37℃ in 5% CO_2 for 2-3 days until 70%-80% CPE, supernatant was discarded, and wells were washed twice with PBS. Using ice-cold 70% acetone (100 μL for each well), the cells were fixed and subsequently stained with 0.4% Sulforhodamine B in a solution of 1% acetic acid. The absorbance at 562 nm was recorded using a SpectraMax® i3 microplate reader (Molecular Devices, California, USA) with reference absorbance at 620 nm. Results were transformed into percentages of controls, and percent protection conferred by the test compound in virus-infected cells was calculated using the formula: [(ODt)virus − (ODc)virus] ÷ [(ODc)mock − (ODc)virus] × 100%, where (ODt)virus represents the optical density measured with a given concentration of the test compound in virus-infected cells; (ODc)virus is the optical density of the non-drug-treated, virus-infected control cells; and (ODc)mock is the optical density of the non-infected, non-drug-treated control cells.

Quantitative RT-PCR (RT-qPCR)

Total RNA was extracted from Vero cells using the QIAamp® Viral RNA Mini Kit (Qiagen, California, USA). TaqMan real-time PCR (RT-qPCR) and reverse transcription PCR were performed using the AgPath-ID™ One-Step RT-PCR Reagents (Applied Biosystems, California, USA) on a Bio-Rad CFX96 thermal cycler (Bio-Rad, California, USA). Data were analyzed using the AB 7900HT real-time system software (Life Technologies, California, USA), with all values normalized to GAPDH levels. The following CVB3 5'NCR primers were used: forward primer 5′-GCGATTGTCACCATWAGCAGYCA-3,' reverse primer 5′-GGCCCCTGAATGCGGCTAATCC-3,' and probe primer 5′-CCGACTACTTTGGGWGTCCGTGT-3'. The following *GAPDH* primers were used: forward primer 5′-GGTCTCCTCTGACTTCAACA-3′, reverse primer 5′-AGCCAAATTCGTTGTCATAC-3′, and probe primer 5′-CCCTCAACGACCACTTTGTCAAG-3′.

Immunofluorescence

5×10^5 Vero cells per well were seeded onto a 6-well culture plate. After 24 hours, the cells were infected with CVB3 and treated with 10 μg/mL saucernetin-8 for 24 hours in DMEM containing 1% FBS. Following treatment, the cells were washed with PBS and fixed with 4% paraformaldehyde (T&I Chem, Incheon, Korea) for 15 minutes. Subsequently, they were permeabilized with 0.25% Triton-X 100 (Sigma Aldrich, Massachusetts, USA) and blocked with 1% BSA (MP Biomedicals, California, USA) for 1 hour at 20℃. Next, the cells were stained using anti-VP3 antibody (Invitrogen, California, USA, cat. no. PA5-111998) as the primary antibody and incubated overnight at 4℃. After washing with PBS, the cells were stained with goat anti-mouse IgG H&L (Alexa Fluor® 647) secondary antibodies (Abcam, Cambridge, United Kingdom) and incubated for 2 hours at 20℃. Following another round of washing with PBS, the cells were stained with 4′,6-diamidino-2-phenylindole (DAPI) and analyzed using an LSM 880 with Airyscan (Zeiss, New York, USA).

mtROS measurement

1×10^6 Vero cells per well were seeded onto a 6-well plate. After 24 hours, the supernatant of each well was replaced with viral infection media containing saucernetin-8. Following a 2-hour incubation, cells were harvested by trypsin-EDTA and stained with Mito-SOX Red (Invitrogen, California, USA), a mitochondrial superoxide indicator, following the manu-

facturer's guidelines. Stained cells were analyzed via FACSVerse (BD Biosciences, New Jersey, USA) without undergoing the formalin fixation step.

Western blot

Total protein lysates from cells were prepared by sonication with PRO-PREP™ Protein Extraction Solution (iNtRON Biotechnology, Seongnam, Korea). The quantification of protein concentrations was conducted with a Pierce™ BCA Protein Assay Kit (Thermo Fisher Scientific, Massachusetts, USA). Uniform protein quantities underwent separation through sodium dodecyl sulfate-polyacrylamide gel electrophoresis and were subsequently transferred onto membranes. The membranes were subsequently incubated with anti-VP3 Abs and anti-β-actin Abs (Santa Cruz Biotechnology, Texas, USA) for 24 hours at 4℃. Thereafter, secondary Abs, goat anti-mouse IgG F(ab′)2, polyclonal Abs (HRP conjugate) (Enzo Life Sciences, New York, USA), were added for 2 hours at 20℃. Proteins were detected using a West Femto Maximum Sensitivity Substrate (Abbkine, Georgia, USA) and visualized with an ImageQuant LAS 4000 mini system (Cytiva, Massachusetts, USA). Chemiluminescence intensity was analyzed using Image J software (NIH, Bethesda, MD, USA).

RESULTS

Antiviral activity of saucenetin-8 isolated from *S. chinensis* against CVB3

To assess the antiviral activity of saucernetin-8, an active compound isolated from *S. chinensis*, against CVB3, we conducted a cell viability assay using Vero cells. Saucernetin-8 exhibited over 60% inhibition of CVB3-induced cytotoxicity at a concentration of 0.4 μg/mL, a level of antiviral activity comparable to that of rupintrivir, a positive control (Fig. 1A). To determine whether saucernetin-8 inhibits CVB3 replication in Vero cells, RT-qPCR was employed. Saucernetin-8 completely suppressed viral genome replication at a concentration of 10 μg/mL. Additionally, it demonstrated over 50% inhibition of viral genome replication at a concentration of 0.4 μg/mL (Fig. 1B). Furthermore, the inhibition of CVB3 capsid protein expression by saucernetin-8 was analyzed via western blot. Results indicated that saucernetin-8 inhibited the expression of VP3, the capsid protein of CVB3, by approximately 50% at a concentration of 10 μg/mL (Fig. 1C). These findings underscore the potential of saucernetin-8 as an effective antiviral agent against CVB3.

Antiviral activity of saucenetin-8 against CVB3 was demonstrated using an immuno-fluorescence assay

To further validate the antiviral activity of saucernetin-8 against CVB3, we conducted confocal microscopy analysis. Immunofluorescent staining of VP3 protein, the capsid protein of CVB3, was performed to evaluate the antiviral activity based on VP3 expression levels in CVB3-infected cells. Vero cells infected with CVB3 were treated with 10 μg/mL of saucernetin-8, and after 24 hours, the expression level of VP3 was assessed. It was observed that saucernetin-8 inhibited VP3 expression by approximately 50% (Fig. 2A, B). These findings, combined with results from previous experiments, indicate the potent antiviral activity of saucernetin-8 against CVB3. Additionally, it effectively suppresses viral replication stage, crucial early steps in the CVB3 life cycle.

Saucernetin-8 triggered the generation of mtROS.

In a study by Song et al., it was reported that lignan compounds, namely manassantin-B and saucerneol, demonstrate antiviral activity against CVB3, EV71, and CVA16 (14, 15). Additionally, these lignan compounds were found to increase mtROS in virus-infected cells. Therefore, in our investigation, we aimed to assess whether saucernetin-8, structurally similar to manassantin-B and saucerneol, influences mtROS production in CVB3-infected Vero cells. CVB3-infected Vero cells were

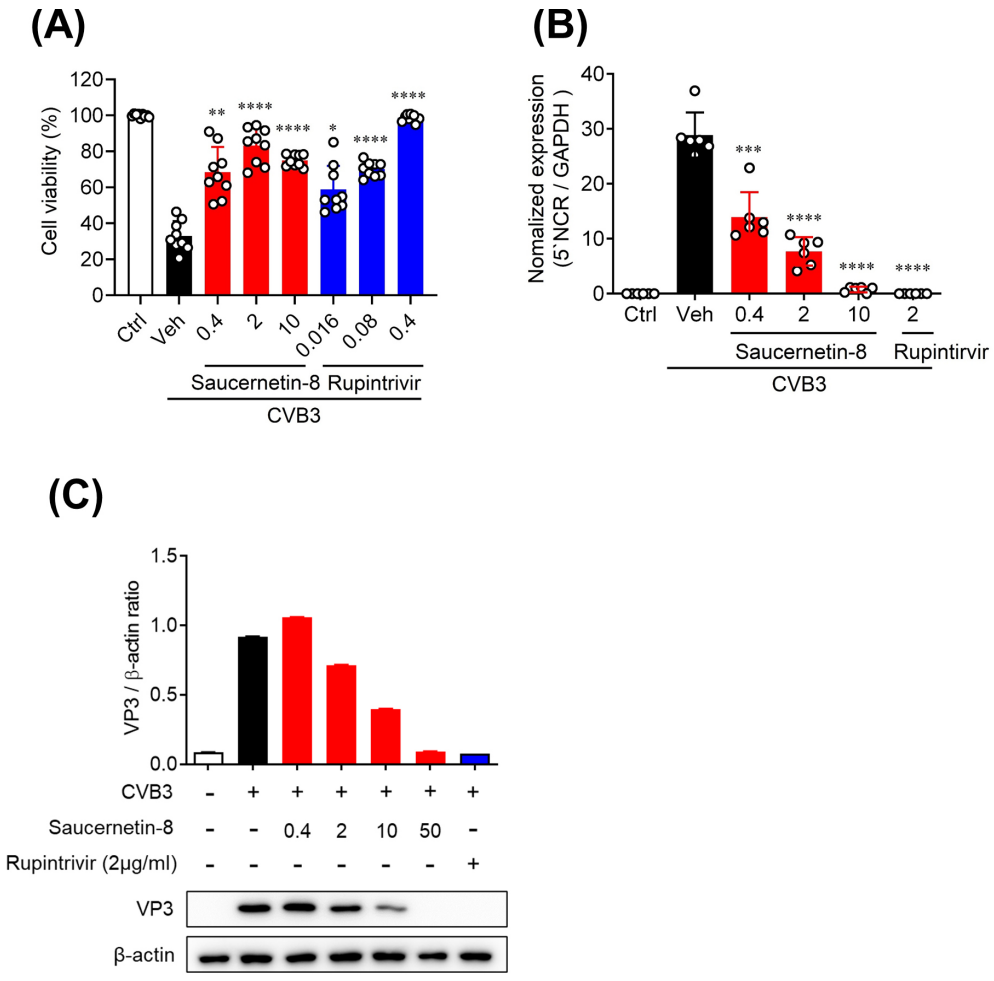

Fig. 1. Antiviral activity of saucernetin-8 against CVB3 *in vitro*. (A) Vero cells were infected with 1 × 10^3 PFU CVB3 and treated with saucernetin-8. Cell viability and cytotoxicity by saucernetin-8 treatment were measured using the sulforhodamine B (SRB) assay. (B) Relative CVB3 5' noncoding region (NCR) gene expression in CVB3-infected Vero cells was determined using RT-qPCR. (C) Western blot analysis of VP3 in CVB3-infected cells after treatment with the vehicle or 0.4 ~ 50 μg/mL of saucernetin-8 for 24 h. The ratio of VP3 to β-actin based on the quantification of bands in the immunoblot. Rupintrivir was used as the positive control. The results are shown as the mean ± SEM. * $p < 0.05$, ** $p < 0.01$, *** $p < 0.001$, and **** $p < 0.0001$ for comparison with the CVB3-infected vehicle-treated group (Veh) based on One-way ANOVA with Bonferroni's multiple comparison test.

treated with saucernetin-8, and mtROS levels were measured via flow cytometry after 2 hours. Our results revealed that treatment with saucernetin-8 increased mitochondrial mtROS levels in CVB3-infected Vero cells. Specifically, while similar levels of mtROS were observed in normal Vero cells and CVB3-infected Vero cells, treatment with saucernetin-8 led to an approximately 30% increase in mtROS levels in both normal and infected Vero cells (Fig. 3A, B). These findings suggest a close association between the antiviral activity of saucernetin-8 against CVB3 and the elevation of mtROS levels.

Saucernetin-8 activated the STING pathway in CVB3-infected cells.

Aberrant cytoplasmic DNA molecules trigger double-stranded DNA-sensing processes, subsequently inducing interferon (IFN) and IFN-stimulated gene (ISG) expression (16). Cytoplasmic mitochondrial DNA (mtDNA) can be recognized by cyclic GMP-AMP synthase (cGAS), thereby activating the STING/TBK1/IRF3 pathway, an innate antiviral immunity pathway (14,

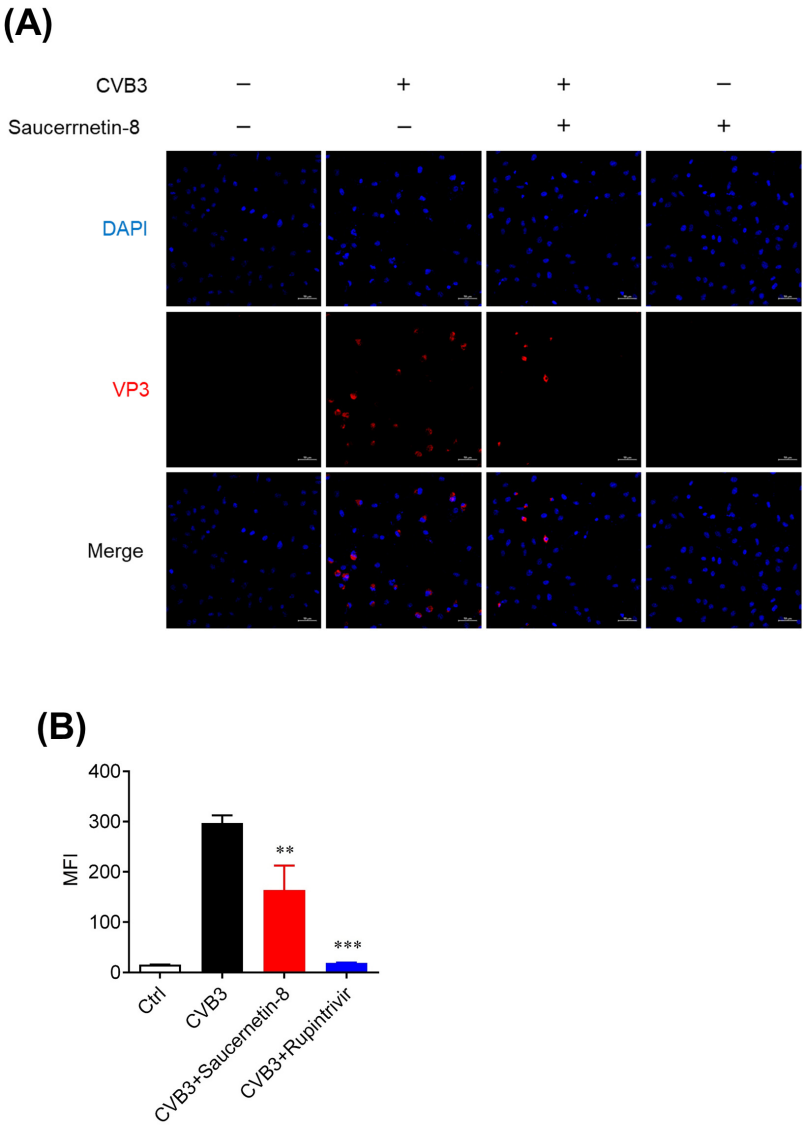

Fig. 2. Antiviral effect of saucernetin-8 confirmed using immunofluorescence. (A) Representative image of VP3 staining in CVB3-infected and uninfected Vero cells treated with 10 μg/mL of saucernetin-8 for 24 h. The image was observed under a confocal microscope. Red signals represent VP3; blue signals represent DAPI-stained nuclei. Scale bar, 50 μm. (B) MFI values of immunofluorescence images were quantified using ZEN software. The results are shown as mean ± SEM. ** $p < 0.01$, and *** $p < 0.001$ for comparison with the CVB3-infected vehicle-treated group (Veh) based on one-way ANOVA with Bonferroni's multiple comparison test.

15, 17, 18). This study employed Western blot analysis to confirm whether the STING pathway was activated by mtROS induced by saucernetin-8. After treating CVB3-infected Vero cells with saucernetin-8 for 24 hours, the expression levels of STING, p-STING, IRF3, and p-IRF3 were examined via Western blotting. Saucernetin-8-treated Vero cells were compared to untreated Vero cells and CVB3-infected Vero cells. The expression levels of STING/p-STING/IRF3/p-IRF3 were found to be significantly elevated in both saucernetin-8-treated Vero cells and CVB3-infected Vero cells compared to the virus-infected control group, as normalized to β-actin levels (Fig. 4A, B). These results suggest that the STING/IRF3 pathway is activated in cells treated with saucernetin-8, which exhibits potent antiviral activity against CVB3.

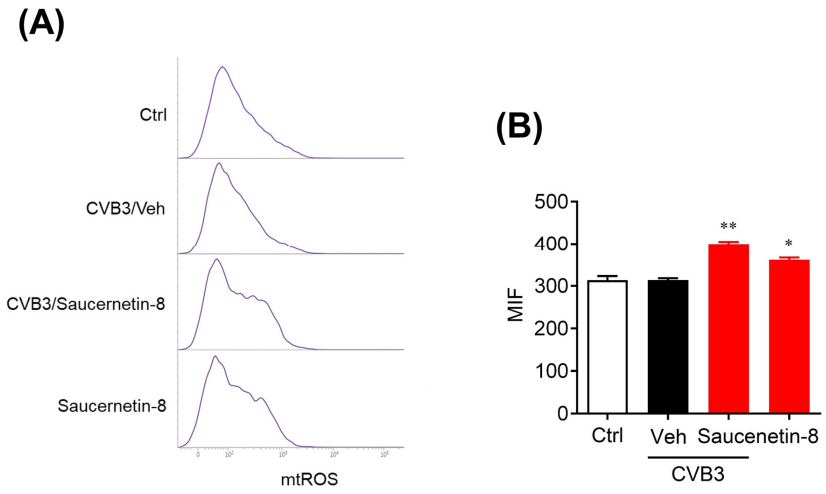

Fig. 3. Saucernetin-8 induced mitochondrial ROS. (A) CVB3-infected Vero cells were treated with 10 μg/mL of saucernetin-8. After 2 h of infection and treatment, harvested cells were stained with 5 μM of Mito-SOX Red reagent and analyzed using fluorescence-activated cell sorting (FACS) to detect reduction in mitochondrial ROS. (B) The mean Mito-SOX Red fluorescence index (MFI) was measured. The results are shown as mean ± SEM. * $p < 0.05$, and ** $p < 0.01$ for comparison with each group based on one-Way ANOVA with Bonferroni's multiple comparison test.

DISCUSSION

Saucernetin-8, a lignan compound isolated from S. *chinensis*, has limited known pharmacological activity compared to other lignan compounds from the same source. However, this study confirms saucernetin-8 as a potent antiviral compound against CVB3 *in vitro*. Currently, there are no clinically approved antiviral drugs for CVB3-induced myocarditis, highlighting the urgent need to develop new antiviral agents against this virus.

Prevention and treatment options for coxsackievirus infections are currently limited. Various vaccine platforms have been developed over the past two centuries, including live attenuated vaccines, inactivated vaccines, subunit vaccines, viral and bacterial vector vaccines, and nucleic acid vaccines (19, 20). However, due to the RNA nature of CVB and its propensity for mutations, along with challenges in immunological cross-reactivity among serotypes, vaccine production remains challenging (14, 20).

Ribavirin, a broad-spectrum nucleoside analog with activity against some viruses, such as hepatitis C virus (21), showed only minor effects on CVB3 infection in Vero cells. Pleconaril, a well-studied anti-enterovirus drug developed to treat colds caused by human rhinoviruses or prevent asthma exacerbations, interacts with the capsid of picornaviruses to inhibit viral attachment and uncoating. However, due to inconsistent results in treating enterovirus infections and limited efficacy against the common cold caused by HRV, clinical development of pleconaril was halted in 2002 (22-27). Rupintrivir, a 3C protease inhibitor of enteroviruses, exhibits broad-spectrum antiviral activity against members of the *Picornaviridae* family. Nevertheless, resistance mutations have been identified in the 3C protease of enterovirus D68, limiting its effectiveness (28-31).

It has been reported that mtROS can disrupt the stability of mitochondrial transcription factor A (TFAM) and mtDNA, leading to the cytoplasmic release of mtDNA and mitochondrial dysfunction (32). Abnormal double-stranded DNA generated in the cytoplasm through viral infection or cellular stress triggers cytoplasmic cyclic GMP-AMP synthase (cGAS) catalyzing cGAMP synthesis, which in turn activates STING (33, 34). Upon activation, STING translocates sequentially from the endoplasmic reticulum (ER) to the ER-Golgi intermediate compartment (ERGIC) to the Golgi apparatus. Activated

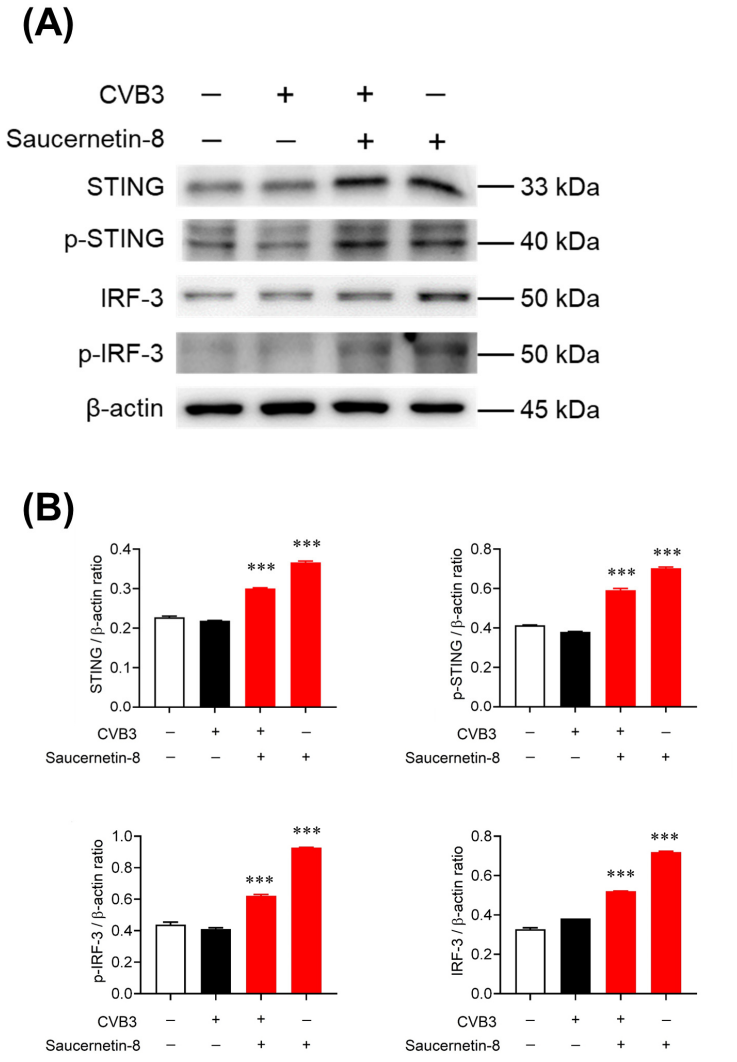

Fig. 4. Saucerneol induced the STING/IRF3 signaling pathway in CVB3-infected cells. (A) Representatives immunoblot results of STING, p-STING, IRF3, p-IRF3, and β-actin to evaluate the activation of their expression in CVB3-infected or uninfected Vero cells after treatment with saucernetin-8 (10 μg/mL). The samples were derived from the same experiment, and gels/blots were processed in parallel. (B)The ratio of STING, p-STING, IRF3, p-IRF3 to β-actin based on the quantification of bands in the immunoblot. The results are shown as the mean ± SEM. *** $p < 0.001$ for comparison with the CVB3-infected vehicle-treated group (Veh) based on One-Way ANOVA with Bonferroni's multiple comparison test.

STING recruits TBK1 to form a translocation complex (35, 36). IRF3 and TBK1 bind to the polymerized STING complex, and phosphorylated IRF3 dissociates from the complex, translocating to the nucleus. There, it promotes the expression of type I interferon (IFN) genes and pro-inflammatory cytokines through the TBK1-IRF3 axis and NF-κB signaling pathway (37-39). Proper activation of this IFNAR signaling cascade is crucial for controlling viral replication during CVB3 infection (40).

In this study, saucernetin-8 demonstrated potent antiviral activity against CVB3, inhibiting over 60% of virus replication at a concentration of 0.4 μg/mL. Moreover, saucernetin-8 significantly increased mtROS in CVB3-infected Vero cells, leading to notable phosphorylation of STING and IRF3, thereby activating gene expression and inhibiting CVB3. Therefore, our findings suggest that the antiviral activity induced by saucernetin-8 is associated with the generation of mtROS and activation of the STING/IRF3 pathway, leading to the activation of type I IFN signaling. Moving forward, we plan to

continuously evaluate the applicability of such strategies in antiviral drug development and continue to develop candidate antiviral agents through compound screening targeting mitochondrial damage.

CONFLICT OF INTEREST

No conflicts of interest related with this article were existed.

ACKNOWLEDGEMENTS

This work was supported by Youngsan University Research Fund of 2023

REFERENCES

1) Zhu P, Ji W, Li D, Li Z, Chen Y, Dai B, et al. Current status of hand-foot-and-mouth disease. *J Biomed Sci* 2023;30:15.

2) Nayak G, Bhuyan SK, Bhuyan R, Sahu A, Kar D, Kuanar A. Global emergence of Enterovirus 71: a systematic review. *Beni Suef Univ J Basic Appl Sci* 2022;11:78.

3) Cooper LT, Jr. Myocarditis. *N Engl J Med* 2009;360:1526-38.

4) Fairweather D, Stafford KA, Sung YK. Update on coxsackievirus B3 myocarditis. *Curr Opin Rheumatol* 2012; 24:401-7.

5) Rose NR. Viral myocarditis. *Curr Opin Rheumatol* 2016;28:383-9.

6) Huber SA. Viral Myocarditis and Dilated Cardiomyopathy: Etiology and Pathogenesis. *Curr Pharm Des* 2016;22:408-26.

7) Lim BK, Yun SH, Ju ES, Kim BK, Lee YJ, Yoo DK, et al. Soluble coxsackievirus B3 3C protease inhibitor prevents cardiomyopathy in an experimental chronic myocarditis murine model. *Virus Res* 2015;199:1-8.

8) Kasai S, Shimizu S, Tatara Y, Mimura J, Itoh K. Regulation of Nrf2 by Mitochondrial Reactive Oxygen Species in Physiology and Pathology. *Biomolecules* 2020;10:320.

9) Ristow M, Zarse K. How increased oxidative stress promotes longevity and metabolic health: The concept of mitochondrial hormesis (mitohormesis). *Exp Gerontol* 2010;45:410-8.

10) Foo J, Bellot G, Pervaiz S, Alonso S. Mitochondria-mediated oxidative stress during viral infection. *Trends Microbiol* 2022;30:679-92.

11) Kopustinskiene DM, Bernatoniene J. Antioxidant Effects of Schisandra chinensis Fruits and Their Active Constituents. *Antioxidants (Basel)*. 2021;10:620.

12) Nowak A, Zakłos-Szyda M, Błasiak J, Nowak A, Zhang Z, Zhang B. Potential of Schisandra chinensis (Turcz.) Baill. in Human Health and Nutrition: A Review of Current Knowledge and Therapeutic Perspectives. *Nutrients* 2019;11:333.

13) Panossian A, Wikman G. Pharmacology of Schisandra chinensis Bail.: an overview of Russian research and uses in medicine. *J Ethnopharmacol* 2008;118:183-212.

14) Song JH, Ahn JH, Kim SR, Cho S, Hong EH, Kwon BE, et al. Manassantin B shows antiviral activity against coxsackievirus B3 infection by activation of the STING/TBK-1/IRF3 signalling pathway. *Sci Rep* 2019;9:9413.

15) Song JH, Mun SH, Yang H, Kwon YS, Kim SR, Song MY, et al. Antiviral Mechanisms of Saucerneol from Saururus

chinensis against Enterovirus A71, Coxsackievirus A16, and Coxsackievirus B3: Role of Mitochondrial ROS and the STING/TKB-1/IRF3 Pathway. *Viruses* 2023;16:16.

16) Lin Y, Zheng C. A Tug of War: DNA-Sensing Antiviral Innate Immunity and Herpes Simplex Virus Type I Infection. *Front Microbiol* 2019;10:2627.

17) Franz KM, Neidermyer WJ, Tan YJ, Whelan SPJ, Kagan JC. STING-dependent translation inhibition restricts RNA virus replication. *Proc Natnal Acad Sci U S A* 2018;115:E2058-e67.

18) Riley JS, Quarato G, Cloix C, Lopez J, O'Prey J, Pearson M, et al. Mitochondrial inner membrane permeabilisation enables mtDNA release during apoptosis. *EMBO J* 2018;37:e99238.

19) Pollard AJ, Bijker EM. A guide to vaccinology: from basic principles to new developments. *Nat Rev Immunol* 2021;21:83-100.

20) Ghattas M, Dwivedi G, Lavertu M, Alameh MG. Vaccine Technologies and Platforms for Infectious Diseases: Current Progress, Challenges, and Opportunities. *Vaccines* 2021;9:1490.

21) Crotty S, Maag D, Arnold JJ, Zhong W, Lau JY, Hong Z, et al. The broad-spectrum antiviral ribonucleoside ribavirin is an RNA virus mutagen. *Nat Med* 2000;6:1375-9.

22) Kaiser L, Crump CE, Hayden FG. In vitro activity of pleconaril and AG7088 against selected serotypes and clinical isolates of human rhinoviruses. *Antiviral Res* 2000;47:215-20.

23) Pevear DC, Tull TM, Seipel ME, Groarke JM. Activity of pleconaril against enteroviruses. *Antimicrob Agents Chemother* 1999;43:2109-15.

24) Rogers JM, Diana GD, McKinlay MA. Pleconaril. A broad spectrum antipicornaviral agent. *Adv Exp Med Biol* 1999;458:69-76.

25) Florea NR, Maglio D, Nicolau DP. Pleconaril, a novel antipicornaviral agent. *Pharmacotherapy* 2003;23:339-48.

26) Romero JR. Pleconaril: a novel antipicornaviral drug. *Expert Opin Investig Drugs* 2001;10:369-79.

27) Senior K. FDA panel rejects common cold treatment. *Lancet Infect Dis* 2002;2:264.

28) Binford SL, Maldonado F, Brothers MA, Weady PT, Zalman LS, Meador JW, 3rd, et al. Conservation of amino acids in human rhinovirus 3C protease correlates with broad-spectrum antiviral activity of rupintrivir, a novel human rhinovirus 3C protease inhibitor. *Antimicrob Agents Chemother* 2005;49:619-26.

29) Matthews DA, Dragovich PS, Webber SE, Fuhrman SA, Patick AK, Zalman LS, et al. Structure-assisted design of mechanism-based irreversible inhibitors of human rhinovirus 3C protease with potent antiviral activity against multiple rhinovirus serotypes. *Proc Natl Acad Sci U S A* 1999;96:11000-7.

30) Patick AK, Binford SL, Brothers MA, Jackson RL, Ford CE, Diem MD, et al. In vitro antiviral activity of AG7088, a potent inhibitor of human rhinovirus 3C protease. *Antimicrob Agents Chemother* 1999;43:2444-50.

31) Sun L, Meijer A, Froeyen M, Zhang L, Thibaut HJ, Baggen J, et al. Antiviral Activity of Broad-Spectrum and Enterovirus-Specific Inhibitors against Clinical Isolates of Enterovirus D68. *Antimicrob Agents Chemother* 2015;59:7782-5.

32) Zhao M, Wang Y, Li L, Liu S, Wang C, Yuan Y, et al. Mitochondrial ROS promote mitochondrial dysfunction and inflammation in ischemic acute kidney injury by disrupting TFAM-mediated mtDNA maintenance. *Theranostics* 2021;11:1845-63.

33) Zhang C, Shang G, Gui X, Zhang X, Bai XC, Chen ZJ. Structural basis of STING binding with and phosphorylation by TBK1. *Nature* 2019;567:394-8.

34) Li T, Chen ZJ. The cGAS-cGAMP-STING pathway connects DNA damage to inflammation, senescence, and cancer. *J Exp Med* 2018;215:1287-99.

35) Ishikawa H, Barber GN. STING is an endoplasmic reticulum adaptor that facilitates innate immune signalling. *Nature* 2008;455:674-8.

36) Hiller B, Hornung V. STING Signaling the enERGIC Way. *Cell host Microbe* 2015;18:137-9.

37) Yum S, Li M, Chen ZJ. Old dogs, new trick: classic cancer therapies activate cGAS. *Cell Res* 2020;30:639-48.

38) Tanaka Y, Chen ZJ. STING specifies IRF3 phosphorylation by TBK1 in the cytosolic DNA signaling pathway. *Sci Signal* 2012;5:ra20.

39) Stetson DB, Medzhitov R. Recognition of cytosolic DNA activates an IRF3-dependent innate immune response. *Immunity* 2006;24:93-103.

40) Schoggins JW. Interferon-Stimulated Genes: What Do They All Do? *Annu Rev Virol* 2019;6:567-84.

Supplementary

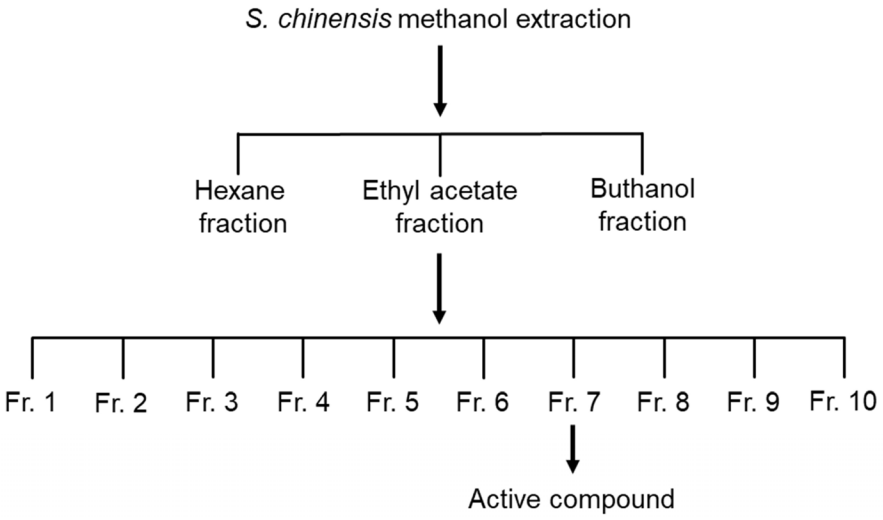

Supplementary Fig. 1. Isolation and purification of active compound.

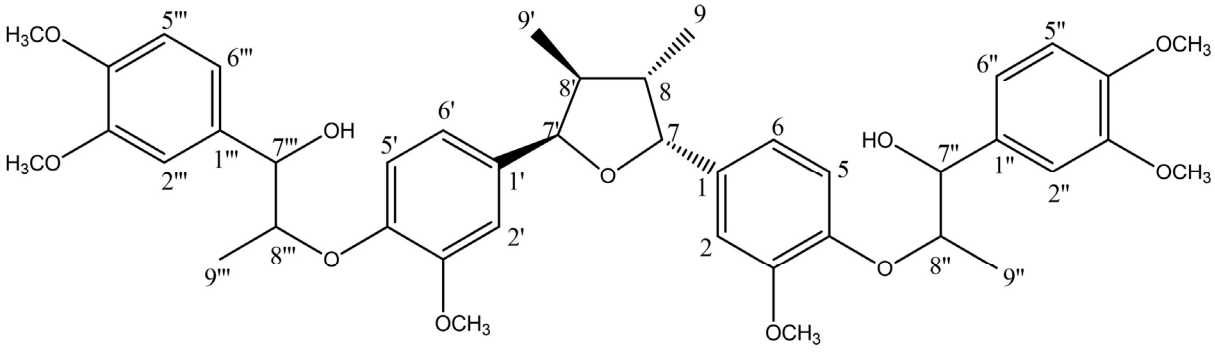

Supplementary Fig. 2. Structure of saucernetin-8.